

Paper-based electrode assemble for impedimetric detection of miRNA

Ece Eksin ^{1,‡}, Hilal Torul ^{2,‡}, Ece Yarali ^{1,‡}, Ugur Tamer^{2,*},

Pagona Papakonstantinou³ and Arzum Erdem ^{1,*}

¹ Department of Analytical Chemistry, Faculty of Pharmacy, Ege University, Bornova, 35100 İzmir, Turkey

² Department of Analytical Chemistry, Faculty of Pharmacy, Gazi University, Etiler, 06330, Ankara, Turkey

³ School of Engineering, Engineering Research Institute, Ulster University, Newtownabbey BT37 0QB, United Kingdom

‡ *These authors contributed equally to this work.*

*Corresponding author (Arzum Erdem): arzum.erdem@ege.edu.tr and arzume@hotmail.com

**Co-corresponding author (Ugur Tamer): utamer33@yahoo.com

Abstract

In the present work, a paper-based electrode assemble was developed and implemented to detect target microRNA 155 (miRNA 155) via electrochemical impedance spectroscopy (EIS) measurements. In this concept, gold nanoparticles (AuNPs) modified paper based electrode assemble system (AuNP-PE) was designed, and characterized by scanning electron microscopy (SEM), cyclic voltammetry (CV) and EIS measurements. The impedimetric detection of miRNA 155 was performed by measuring the fractional change at the charge transfer resistance (R_{ct}). The detection limits were found as 33.8 nM in PBS and 93.4 nM in fetal bovine serum (FBS) medium, respectively. The selectivity of the proposed assay was tested against to non-complementary (NC) and mismatch (MM) miRNA sequences in the presence of mixture sample containing miRNA:NC (1:1) and miRNA:MM (1:1) in PBS (pH 7.40) or FBS. The analytical performance and the selectivity of impedimetric biosensor were also tested in FBS.

Keywords: paper based electrode; microRNA; gold nanoparticles; electrochemical impedance spectroscopy.

31 **1. Introduction**

32 microRNAs have significant roles in the regulation of differentiation, angiogenesis,
33 proliferation, immune cell function, wound healing and apoptosis [1-4]. Especially the level of
34 expression of Circulating miRNAs is tissue specific and have potential for use as biomarkers
35 [2,3]. The overexpression of miRNA-155, which is known as a significant circulating miRNA,
36 can be used as a biomarker for diagnosis and progression of cancers [5,6]. microRNAs detection
37 in biological systems is still challenging [7-9] and upto date, several methods are reported s
38 for miRNA detection such as RT-PCR [10-12], microarray technique [13,14], northern blotting
39 [15,16], and in situ hybridization [17-19]. In spite of the advantages, these methods require
40 expensive instruments and reagents, labelled miRNAs, high sample volumes and relatively pure
41 miRNA samples [20]. Therefore, it is extremely important that miRNA detection methods
42 should be simple, fast and label-free [21]. At this juncture, electrochemical techniques have
43 received notable attention due to their easy controllability, good stability, reproducibility,
44 sensitiveness and cost-effectiveness [22].

45 Currently, various nanostructure-based sensing platforms have been employed in constructing
46 DNA sensors owing to nanomaterial's unique advantages (e.g., large surface areas, unique
47 properties such as mechanical, electronic and catalytic) [23]. Among the nanomaterials, gold
48 nanoparticles (AuNPs) have become interesting option for biomedical use due to their several
49 kinds of effective properties [24,25]. In contrast to the graphene and iron oxides, the high
50 affinity of the gold-sulfur bonding and other unique properties, such as high conductivity and
51 large surface [26-28]. AuNPs, with the diameter of 1-100 nm, have high surface-to-volume
52 ratio and high surface energy to provide a stable immobilization of a large amount of
53 biomolecules retaining their bioactivity. Additionally, AuNPs are able to allow fast and direct
54 electron transfer between electroactive species and electrode materials [29]. A label-free and
55 simple electrochemical microRNA biosensor was developed by Tian et al. (2018). Toluidine
56 blue (TB) and AuNPs superlattice were used as a redox indicator and support material,
57 respectively. The polypyrrole coated AuNPs was self-assembled n order to obtain the maximum
58 current. Under optimum conditions, the hybridization of single strand RNA probe with the
59 miRNA target sequence were monitored using CV and differential pulse voltammetry (DPV)
60 by measuring the peak current of TB [29]. In another work, DNA hybridization was investigated
61 using AuNPs and DNA immobilized GCE. Thiol linked probe was immobilized onto GCE and
62 the hybridization of probe and target DNA was examined using DPV technique by measuring

63 the Methylene blue signal [30]. A simple filtration based assay in order to develop paper based
64 biosensor was performed by Tian et al. [31] for simultaneous detection of miRNA 144 and
65 miRNA 21. MOF conjugated bio-probe, methylene blue (MB) and ferrocene (Fc) were used for
66 contribution of sensor sensitivity [31].

67 Polymers and paper are commonly used flexible substrates for the development of bioanalytical
68 devices [8,9,32-35]. Particularly, paper is flexible, widely available, cost-effective, hydrophilic,
69 easy to demolish and biocompatible. Therefore, it is a convenient substrate for biosensors.
70 Additionally, the adsorption of biomolecules or nanoparticles can be performed easily due to
71 the porosity of the paper surface [32-35]. Paper based microfluidic electrochemical DNA
72 biosensor was developed for the detection of Epidermal growth factor receptor (EGFR)
73 mutations in saliva samples by Tian et al. (2017). ssDNA was adsorbed onto the surface of
74 polypyrrole membran modified Au electrode, and the electrochemical signals were obtained.
75 The horseradish peroxidase (HRP) recognized the methylene blue labeled DNA and showed
76 unique electrocatalytic behavior to H₂O₂ [36]. In another study, paper-based analytical devices
77 (μ PADs) in combination with screen printed electrodes were developed by Lu et al. (2012).
78 Thionine (TH) bound to double strand DNA (TH/D1) and complementary ssDNA (S3)
79 immobilized on nanoporous gold (NPG) and formed S3-TH/D1-NPG conjugates. The designed
80 μ PADs nucleic acid sensor showed good performance in human serum assay [37].

81 To best of our knowledge, AuNPs modified paper electrode assemble system (AuNP-PE) was
82 developed and applied for the first time herein for impedimetric detection of miRNA 155. After
83 thiol linked DNA probe immobilization on AuNP-PE, its complementary target miRNA was
84 recognized by capturing probe at the electrode surface during hybridization process. The
85 selectivity of paper based biosensor specific to target miRNA (i.e, miRNA 155) was tested
86 against to non-complementary (NC) and mismatch (MM) miRNA sequences, in the presence
87 of mixture samples containing miRNA:NC (1:1) and miRNA:MM (1:1). In addition, the
88 analytical performance and the selectivity of impedimetric biosensor were also tested in fetal
89 bovine serum (FBS) medium.

90

91

92

93

94 **2. Experimental**

95 ***2.1. Instruments***

96 Electrochemical measurements were performed with AUTOLAB-302 PGSTAT with NOVA
97 (version 1.1.2 Eco Chemie, The Netherlands) software package (Eco Chemie, The Netherlands)
98 in a Faraday cage.

99 ***2.2. Chemicals***

100 Carbon paste was purchased from Daejoo Electronic Materials (Shanghai, South Korea).
101 Silver/Silver chloride (Ag/AgCl) paste was purchased from Gwent Group (Torfaen, UK). The
102 miRNA-155 specific DNA probe, miRNA-155 target and the other oligonucleotides (see
103 supporting information for more information) were purchased from TIB Molbiol (Germany).
104 All other chemicals were purchased from Sigma and Merck.

105 ***2.3. Fabrication of paper based electrodes***

106 The most proper construction was provided using NC membrane as a structure. The printing of
107 the hydrophobic barriers was occurred onto the NC membrane surface by using a wax printer
108 (XEROX ColorQube™ 8570 (Norwalk, USA) after designing a pattern which includes a
109 microfluidic channel and a working area. To provide capillary flow, channels were designed
110 with a diameter of 2 mm and a length of 1.5 cm. In the present work, electrodes are placed in
111 the working area and this area was designed as about 20 mm² with 270 angles to provide the
112 maximum spread speed of liquid. The fabrication process of a paper electrode is shown in Fig.
113 S1.

114 ***2.4. Design of the electrochemical detector of paper based electrode***

115 To build the electrodes onto the patterned NC membrane, an additional pattern was drawn on a
116 steel wafer with 1 mm thickness. Then the obtained pattern was cut by laser cutter. Resulted
117 mask was placed on the working area of the NC membrane and carbon ink was applied to give
118 shape as the working (WE) and counter electrode (CE). Additionally, we used Ag/AgCl ink to
119 create the reference electrode (RE). Conductive pads were created by using copper wire. Before
120 attaching the copper wire, wax printed NC membrane with electrodes was backed at 100 °C for
121 5 min to let carbon ink fix on the NC membrane surface and also the wax melt and interpenetrate
122 through the NC membrane. The electrode design is schematized in Fig. S2. The storage stability
123 of the paper electrodes was evaluated and the results are given in Fig. S3.

124 ***2.5.Preparation of AuNPs modified electrodes***

125 AuNPs were deposited onto PE using chronoamperometry in 15 mM HAuCl₄ gold precursor
126 aqueous solution. 5 μL of HAuCl₄ solution was dropped onto the PE and -0.3 V constant
127 potential is applied during 600 s.

128 ***2.6.Probe immobilization on AuNPs modified electrodes***

129 5 μL of thiol liked miRNA-155 DNA probe is dropped and allowed to immobilize onto the
130 AuNP-PE during 10 min. Then, washed with PBS (pH 7.40).

131 ***2.7.Hybridization of probe and miRNA-155***

132 5 μL of miRNA-155 target in various concentrations were applied to the electrode and washed
133 with PBS (pH 7.40) after 5 min of incubation at room temperature.

134 ***2.8.Impedimetric measurement***

135 20 μL of 0.1 M KCl solution containing 5 mM [Fe(CN)₆]^{3-/4-} was dropped into the paper
136 electrochemical cell through the channel.

137

138

139

140

141

142

143

144

145

146

147

148

149

150 **3. Results and Discussion**

151 ***3.1. Microscopic and electrochemical characterization of modified/unmodified***
152 ***electrodes***

153 Scanning electron microscopy (SEM) was used to characterize AuNPs modified paper based
154 electrode. AuNPs were deposited on the working electrode surface by electrochemical
155 reduction. While Fig. 1a,b show bare carbon paste PE at different magnification levels, Fig.
156 1c,d show AuNPs deposited on PE surface. AuNPs were homogeneously distributed on the PE
157 surface as shown in Fig. 1c,d. The average diameter of AuNPs was calculated as 262 ± 30 nm.

158
159 **Figure 1**

160
161 In order to explore the electrochemical behavior of PE and AuNPs modified PE, cyclic
162 voltammetry was performed. The anodic and cathodic currents; I_a , I_c , relative charge; Q (C),
163 and the surface areas of the PE and AuNPs modified PE are shown in Table S1. The I_c and I_a
164 of AuNPs modified PE (Fig. 2-I) were much larger than I_c and I_a of PE (Fig. 2-I). These results
165 confirmed that the accelerated electron transfer occurred by means of AuNPs [38]. The
166 electroactive surface areas (A) of PE and AuNPs-PE were calculated [39] as 0.019 cm^2 and
167 0.037 cm^2 respectively. In comparison to the calculated surface area of PE, an increase about
168 91 % at surface area of AuNP-PE was obtained by means of conductive behavior of AuNPs
169 [38].

170
171 **Figure 2.**

172
173 EIS was also performed in order to obtain detailed information regarding modification process
174 since measurements carried out in the absence/presence of AuNP modification (Fig. 2-II). The
175 change in the value of R_{ct} was associated with the modification processes of PE surface. The
176 measured R_{ct} of unmodified PE was 7122.75 ± 440 Ohm (RSD %, 6.18 %, $n=4$). After
177 modification of AuNP, the R_{ct} exhibited a substantial decrease (161 folds) and measured as
178 44.12 ± 3.76 Ohm (RSD %, 8.53 %, $n=4$). This observation indicates that the AuNPs with high

179 conductivity acted as a conductive layer for the charge transfer. These results are in good
180 consistent with the CV results presented in this present study.

181 *Analytical performance*

182 The analytical performance of AuNP-PEs is tested through the detection of miRNA-155 target
183 at different concentrations. Shown in Fig. 3, with the increase of miRNA-155 target
184 concentration, the R_{ct} value increases over a wide concentration range of 0 – 1.5 $\mu\text{g/mL}$ and
185 then decrease in the presence of 2 $\mu\text{g/mL}$ miRNA-155 target as shown in Fig. S4. The linear
186 regression equation was $R_{ct} (\text{Ohm}) = 16.57 [\text{miRNA-155}] (\mu\text{g/mL}) + 8.02$ with a correlation
187 coefficient of 0.98 and the limit of detection (LOD) was calculated as 0.25 $\mu\text{g/mL}$ (33.8 nM)
188 [40].

189 **Figure 3.**

190

191 *3.2.Selectivity of the AuNPs modified electrodes*

192 To evaluate the specificity of the AuNP-PE, the interference effect of the noncomplementary
193 and single base mismatched strands were also investigated. The efficiency of hybridization (HE
194 %) is used as the evidence of the hybridization effectiveness [41] and the average R_{ct} values
195 with the HE % can be seen in Table S2. HE % is accepted as 100 % for hybridization between
196 probe and miRNA 155. The results clearly reveal that the AuNP-PE showed a sensitive
197 behavior to its complementary target.

198

199 **Figure 4.**

200

201 *3.3.Analytical performance in serum media*

202 In the present study, the analytical performance of AuNP-PEs was tested in serum media (Fig.
203 5). When the hybridization was performed in case of the increasing concentration of miRNA-
204 155 target, the R_{ct} value increased among the concentration range of 0 – 4 $\mu\text{g/mL}$, then
205 decreased in the presence of 6 $\mu\text{g/mL}$ miRNA-155 target (Fig. S5). The linear regression
206 equation was $R_{ct} (\text{Ohm}) = 11.15 [\text{miRNA-155}] (\mu\text{g/mL}) + 36$ with $R^2=0.98$ and the LOD was
207 calculated as 0.69 $\mu\text{g/mL}$ (93.4 nM).

208 **Figure 5.**

209

210 ***3.4.Selectivity in serum media***

211 The specificity of the AuNP-PE in serum media was then tested (Fig. S6). The HE %s were
212 calculated as 13 % and 16 %, in case of possible hybridization/interaction between probe and
213 NC, MM, respectively. On the other hand, HE %s were 65 % and 41 %, respectively after
214 hybridization of probe and miR-155 target in the presence of NC or MM (Table S3).

215 According to our results related to the selectivity test in buffer and serum media, it can be said
216 that the proposed AuNP-PEs exhibited more selective behavior in complex serum medium than
217 buffer. These results showed that AuNP-PEs are able to perform microRNA detection in a
218 sensitive and selective way even in a complex medium as serum.

219 Storage stability of the paper electrodes was evaluated. Fig. S3 shows the stability of the
220 electrodes during 60 days of storage in dark conditions and without other special care.

221 Several reports related to the electrochemical detection of miRNAs were summarized in Table
222 S4 [29,41-61]. In the present work, the impedimetric miRNA-155 analysis was accomplished
223 in relatively shorter time (i.e 15 min) compared to earlier works shown in Table S4. The
224 detection limit was found respectively to be 33.8 nM in PBS and 93.4 nM in FBS:PBS (1:1)
225 diluted solution, which was comparable to earlier works [42-48] (Table S4).

226

227

228

229

230

231

232

233

234

235 **4. Conclusion**

236 The gold nanoparticles (AuNPs) modified paper based electrode assemble system (AuNP-PE)
237 was designed for the first time in this present study, and successfully applied to perform fast,
238 sensitive, selective and quantitative miRNA-155 detection. Our results showed that the stability
239 of these electrodes during 60 days of storage in dark conditions and without other special care.

240 Since this protocol exhibits more selective behavior in complex serum medium than buffer, it
241 is obvious that AuNP-PEs could be able to perform selectively nucleic acid detection including
242 miRNA, SNP, etc. even in a complex medium as serum.

243 AuNPs-PEs can be assesable as a promising platform for analysis in real serum samples for
244 early diagnosis of cancer. It is important to mention that usage of a paper based microfluidic
245 chip, except for isolation of target analyte from solution, provides us to benefit from the
246 advantages of miniaturized systems comparison to the conventional batch technique.

247

248 **Conflicts of interest**

249 There are no conflicts of interest to declare

250

251 **Acknowledgements**

252 This study was supported under the Newton-Katip Celebi Funding programme and all
253 authors acknowledge the financial support from Turkish Scientific and Technological
254 Research Council (TUBITAK; Project no. 215Z702) and from British Council (Newton
255 fund, Institutional Links, Ref: 216182787). PhD and master students respectively E.E.
256 and E.Y. acknowledge a project scholarship through by project (TUBITAK Project no.
257 215Z702). Authors also acknowledge to helpful discussion of Assoc. Prof. Yildiz
258 Uludag as the project consultant during project (TUBITAK; Project no. 215Z702). A.E.
259 also would like to express her gratitude to the Turkish Academy of Sciences (TUBA) as
260 a Principal member for its partial support.

261

262

263

264

265 **References**

- 266 [1] H.F. Dong, J.P. Lei, L. Ding, Y.Q. Wen, H.X. Ju, X.J. Zhang, microRNA: function,
267 detection, and bioanalysis, *Chem. Rev.* 113 (2013) 6207-6233.
268 <https://doi.org/10.1021/cr300362f>.
- 269 [2] M.S. Ebert, P.A. Sharp, Roles for microRNAs in conferring robustness to biological
270 processes, *Cell* 27 (2012) 515-524. <https://doi.org/10.1016/j.cell.2012.04.005>
- 271 [3] C.A. Andorfer, B.M. Necela, E.A. Thompson, E., A., Perez, MicroRNA signatures: clinical
272 biomarkers for the diagnosis and treatment of breast cancer, *Trends Mol. Med.* 17 (2011) 313-
273 319. <https://doi.org/10.1016/j.molmed.2011.01.006>.
- 274 [4] T. Kilic, A. Erdem, M. Ozsoz, S. Carrara, microRNA biosensors: Opportunities and
275 challenges among conventional and commercially available techniques, *Biosens. Bioelectron.*
276 99 (2018) 525-546. <https://doi.org/10.1016/j.bios.2017.08.007>
- 277 [5] D. Jurkovicova, M. Magyerkova, L. Kulcsar, M. Krivjanska, V. Krivjansky, A. Giba-
278 dulinova, I. Oveckova, M. Chovanec, miR-155 as a diagnostic and prognostic marker in
279 hematological and solid malignancies, *Neoplasma* 61 (2014) 241-251.
280 https://doi.org/10.4149/neo_2014_032
- 281 [6] Y. Sun, M. Wang, G. Lin, S. Sun, X. Li, J. Qi, J., Li, Serum microRNA-155 as a potential
282 biomarker to track disease in breast cancer, *PloS One* 7 (2012) 1-8.
283 <https://doi.org/10.1371/journal.pone.0047003>
- 284 [7] A. Liu, K. Wang, S. Weng, Y. Lei, L. Lin, W. Chen, X. Lin, Y. Chen, Development of
285 electrochemical DNA biosensors, *Trends Anal. Chem.* 37 (2012) 101-111.
286 <https://doi.org/10.1016/j.trac.2012.03.008>
- 287 [8] C. Kokkinos, A. Economou, M.I. Prodromidis, Electrochemical immunosensors: Critical
288 survey of different architectures and transduction strategies, *Trends Anal. Chem.* 79 (2016) 88-
289 105. <https://doi.org/10.1016/j.trac.2015.11.020>
- 290 [9] C. Kokkinos, A. Economou, Emerging trends in biosensing using stripping voltammetric
291 detection of metal-containing nanolabels – A review, *Anal. Chim. Acta* 961 (2017) 12-32.
292 <https://doi.org/10.1016/j.aca.2017.01.016>
- 293 [10] E. Varkonyi-Gasic, R. Wu, M. Wood, E.F. Walton, R.P. Hellens, Protocol: a highly
294 sensitive RT-PCR method for detection and quantification of microRNAs, *Plant Methods* 3
295 (2007) 1-12. <https://doi.org/10.1186/1746-4811-3-12>
- 296 [11] Z. Wang, B. Yang, End-point stem-loop real-time RT-PCR for miRNA quantification, in:
297 Wang, Z., Yang, B., *MicroRNA expression detection methods*. Springer, New York, (2010)
298 131-140. https://doi.org/10.1007/978-3-642-04928-6_5
- 299 [12] Y.K. Ho, W.T. Xu, H.P. Too, Direct Quantification of mRNA and miRNA from Cell
300 Lysates Using Reverse Transcription Real Time PCR: A Multidimensional Analysis of the
301 Performance of Reagents and Workflows, *PloS One* 8 (2013) e72463.
302 <https://doi.org/10.1371/journal.pone.0072463>

- 303 [13] B. Zhao, L. Jin, J. Wei, Z. Ma, W. Jiang, L. Ma, Y. Jin, A simple and fast method for
304 profiling microRNA expression from low-input total RNA by microarray, *IUBMB life* 64
305 (2012) 612-616. <https://doi.org/10.1002/iub.1026>
- 306 [14] R.Q. Liang, W. Li, Y. Li, C.Y. Tan, J.X. Li, Y.X. Jin, K.C. Ruan, An oligonucleotide
307 microarray for microRNA expression analysis based on labeling RNA with quantum dot and
308 nanogold probe, *Nucleic Acids Res* 33 (2005) e17. <https://doi.org/10.1093/nar/gni019>
- 309 [15] É. Várallyay, J. Burgyán, Z. Havelda, MicroRNA detection by northern blotting using
310 locked nucleic acid probes. *Nat. Protoc.* 3 (2008) 190-196.
311 <https://doi.org/10.1038/nprot.2007.528>
- 312 [16] D.C. Rio, Northern blots for small RNAs and microRNAs, *Cold Spring Harbor Protocols*
313 2014, 7, 793-807. <https://doi.org/10.1101/pdb.prot080838>
- 314 [17] R. Song, S. Ro, W. Yan, In situ hybridization detection of microRNAs. *RNA Therapeutics:*
315 *Function, Design, and Delivery*, (2010) 285-292. [https://doi.org/10.1007/978-1-60761-657-](https://doi.org/10.1007/978-1-60761-657-3_18)
316 [3_18](https://doi.org/10.1007/978-1-60761-657-3_18)
- 317 [18] S.C. Doné, O. Beltcheva, In Situ Hybridization Detection of miRNA Using LNA™
318 Oligonucleotides, *RNA Mapping: Methods and Protocols*, (2014) 57-71.
319 https://doi.org/10.1007/978-1-4939-1062-5_6
- 320 [19] X. Zhang, X. Lu, G. Lopez-Berestein, A. Sood, G. Calin, In situ hybridization-based
321 detection of microRNAs in human diseases, *microRNA Diagn Ther* 1 (2013) 12-23.
322 <https://doi.org/10.2478/micrnat-2013-0002>
- 323 [20] Y. Zhou, M. Wang, X. Meng, H. Yin, S. Ai, Amplified electrochemical microRNA
324 biosensor using a hemin-G-quadruplex complex as the sensing element, *RSC Adv.* 2 (2012)
325 7140-7145. <https://doi.org/10.1039/C2RA20487H>
- 326 [21] F. Hakimian, H. Ghourchian, A.S. Hashemi, M.R. Arastoo, M.B. Rad, Ultrasensitive
327 optical biosensor for detection of miRNA-155 using positively charged Au nanoparticles, *Sci.*
328 *Rep.* 8 (2018) 2943. <https://doi.org/10.1038/s41598-018-20229-z>
- 329 [22] T. Hu, L. Zhang, W. Wen, X. Zhang, S. Wang, Enzyme catalytic amplification of miRNA-
330 155 detection with graphene quantum dot-based electrochemical biosensor, *Biosens.*
331 *Bioelectron.* 77 (2016) 451-456. <https://doi.org/10.1016/j.bios.2015.09.068>
- 332 [23] X. Han, X., Fang, A. Shi, J. Wang, Y. Zhang, An electrochemical DNA biosensor based
333 on gold nanorods decorated graphene oxide sheets for sensing platform, *Anal. Biochem.* 443
334 (2013) 117-123. <https://doi.org/10.1016/j.ab.2013.08.027>
- 335 [24] G.M. Zhang, Functional gold nanoparticles for sensing applications, *Nanotechnol. Rev.* 2
336 (2013) 269-288. <https://doi.org/10.1515/ntrev-2012-0088>
- 337 [25] Y. Li, H. J. Schluesener, S. Xu, Gold nanoparticle-based biosensors, *Gold Bulletin* (2010)
338 29-41. <https://doi.org/10.1007/BF03214964>
- 339 [26] C. Deng, J. Chen, Z. Nie, M. Wang, X. Chu, X., Chen, S. Yao, Impedimetric Aptasensor
340 with Femtomolar Sensitivity Based on the Enlargement of Surface-Charged Gold
341 Nanoparticles, *Anal. Chem.* 81 (2008) 739-745. <https://doi.org/10.1021/ac800958a>

- 342 [27] N. German, A. Ramanaviciene, A. Ramanavicius, Formation of Polyaniline and
343 Polypyrrole Nanocomposites with Embedded Glucose Oxidase and Gold Nanoparticles,
344 *Polymers* 11 (2019) 377. <https://doi.org/10.3390/polym11020377>
- 345 [28] N. German, A. Ramanavicius, A. Ramanaviciene, Amperometric Glucose Biosensor
346 Based on Electrochemically Deposited Gold Nanoparticles Covered by Polypyrrole,
347 *Electroanalysis*, 29 (2017) 1267-1277. <https://doi.org/10.1002/elan.201600680>
- 348 [29] L. Tian, K. Qian, J. Qi, Q. Liu, C. Yao, W. Song, Y. Wang, Gold nanoparticles
349 superlattices assembly for electrochemical biosensor detection of microRNA-21, *Biosens.*
350 *Bioelectron.* 99 (2018) 564-570. <https://doi.org/10.1016/j.bios.2017.08.035>
- 351 [30] J. Kang, X. Li, G. Wu, Z. Wang, X. Lu, A new scheme of hybridization based on the Au
352 nano-DNA modified glassy carbon electrode, *Anal. Biochem.* 364 (2007) 165-170.
353 <https://doi.org/10.1016/j.ab.2007.01.037>
- 354 [31] C. Desmet, C.A. Marquette, L.J. Blum, B. Doumeche, Paper electrodes for
355 bioelectrochemistry: Biosensors and biofuel cells, *Biosens. Bioelectron.* 76 (2016) 145-163.
356 <https://doi.org/10.1016/j.bios.2015.06.052>
- 357 [32] R. Tian, Y. Li, J. Bai, Hierarchical assembled nanomaterial paper based analytical devices
358 for simultaneously electrochemical detection of microRNAs, *Anal. Chim. Acta* 1058 (2019)
359 89-96. <https://doi.org/10.1016/j.aca.2019.01.036>
- 360 [33] J. Mettakoonpitak, K. Boehle, S. Nantaphol, P. Teengam, J.A. Adkins, M. Srisa-Art, C.S.
361 Henry, Electrochemistry on Paper-based Analytical Devices: A Review, *Electroanalysis* 28
362 (2016) 1420-1436. <https://doi.org/10.1002/elan.201501143>
- 363 [34] Y. Yang, E. Noviana, M.P. Nguyen, B.J. Geiss, D.S. Dandy, C.S. Henry, Paper-Based
364 Microfluidic Devices: Emerging Themes and Applications, *Anal. Chem.* 89 (2017) 71-91.
365 <https://doi.org/10.1021/acs.analchem.6b04581>
- 366 [35] Y. Xia, J. Si, Z. Li, Fabrication techniques for microfluidic paper-based analytical devices
367 and their applications for biological testing: A review, *Biosens. Bioelectron.* 77 (2016) 774-
368 789. <https://doi.org/10.1016/j.bios.2015.10.032>
- 369 [36] T. Tian, H. Liu, L. Li, J. Yu, S. Ge, X. Song, M. Yan, Paper-based biosensor for
370 noninvasive detection of epidermal growth factor receptor mutations in non-small cell lung
371 cancer patients, *Sens. Act. B* 251 (2017) 440-445. <https://doi.org/10.1016/j.snb.2017.05.082>
- 372 [37] J. Lu, S. Ge, L. Ge, M. Yan, J. Yu, Electrochemical DNA sensor based on three-
373 dimensional folding paper device for specific and sensitive point-of-care testing, *Electrochim.*
374 *Acta* 80 (2012) 334-341. <https://doi.org/10.1016/j.electacta.2012.07.024>
- 375 [38] K.-J. Huang, Y.-J. Liu, H.-B. Wang, Y.-Y. Wang, Y.-M. Liu, Sub-femtomolar DNA
376 detection based on layered molybdenum disulfide/multi-walled carbon nanotube composites,
377 Au nanoparticle and enzyme multiple signal amplification, *Biosens. Bioelectron.* 55 (2014)
378 195-202. <https://doi.org/10.1016/j.bios.2013.11.061>
- 379 [39] T.E. Cummings, P.J. Elving, Determination of the electrochemically effective electrode
380 area, *Anal. Chem.* 50 (1978) 480-488. <https://doi.org/10.1021/ac50025a031>

- 381 [40] J.N. Miller, J.C. Miller, *Statistics and Chemometrics for Analytical Chemistry*, Pearson
382 Educ, London, (2005) pp. 121-123. <https://doi.org/10.1198/tech.2004.s248>
- 383 [41] A. Ganguly, J. Benson, P. Papakonstantinou, Sensitive Chronocoulometric Detection of
384 miRNA at Screen-Printed Electrodes Modified by Gold-Decorated MoS₂ Nanosheets. *ACS*
385 *Appl. Bio Mater.* (2018) 1, 1184-1194. <https://doi.org/10.1021/acsabm.8b00398>
- 386 [42] E. Yarah, E. Kanat, Y Erac, A. Erdem, Ionic Liquid Modified Single-use Electrode
387 Developed for Voltammetric Detection of miRNA-34a and its Application to Real Samples,
388 *Electroanalysis* 32 (2020) 384-393. <https://doi.org/10.1002/elan.201900353>
- 389 [43] A. Erdem, E. Eksin, D. Isin, D., Polat, Graphene Oxide Modified Chemically Activated
390 Graphite Electrodes for Detection of microRNA, *Electroanalysis*, 29 (2017) 1350-1358.
391 <https://doi.org/10.1002/elan.201600761>
- 392 [44] A. Erdem, E. Eksin, G. Congur, Indicator-free electrochemical biosensor for microRNA
393 detection based on carbon nanofibers modified screen printed electrodes. *J. Electroanal. Chem.*
394 755 (2015) 167-173. <https://doi.org/10.1016/j.jelechem.2015.07.031>
- 395 [45] J. Mandli, A. Amine, Impedimetric genosensor for miRNA-34a detection in cell lysates
396 using polypyrrole, *J. Solid State Electrochem.* (2018) 1007-1014.
397 <https://doi.org/10.1007/s10008-017-3819-5>
- 398 [46] D. Isin, E. Eksin, A. Erdem, Graphene oxide modified single-use electrodes and their
399 application for voltammetric miRNA analysis, *Mater. Sci. Eng. C* 75 (2017) 1242-1249.
400 <https://doi.org/10.1016/j.msec.2017.02.166>
- 401 [47] E. Kesici, E. Eksin, A. Erdem, An Impedimetric Biosensor Based on Ionic Liquid-
402 Modified Graphite Electrodes Developed for microRNA-34a Detection, *Sensors* 18 (2018)
403 E2868. <https://doi.org/10.3390/s18092868>
- 404 [48] G. Congur, E. Eksin, A. Erdem, Impedimetric Detection of microRNA at Graphene Oxide
405 Modified Sensors, *Electrochim. Acta* 172 (2015) 20-27.
406 <https://doi.org/10.1016/j.electacta.2015.03.210>
- 407 [49] F. Li, J. Peng, J. Wang, H. Tang, L. Tani Q. Xie, S. Yao, Carbon nanotube-based label-
408 free electrochemical biosensor for sensitive detection of miRNA-24, *Biosens. Bioelectron.* 54
409 (2014) 158-164. <https://doi.org/10.1016/j.bios.2013.10.061>
- 410 [50] M. Bartosik, M. Trefulka, B. Hrstka, B. Vojtesek, E. Palecek, Os(VI)bipy-based
411 electrochemical assay for detection of specific microRNAs as potential cancer biomarkers,
412 *Electrochem. Commun* 33 (2013) 55-58. <https://doi.org/10.1016/j.elecom.2013.04.009>
- 413 [51] D. Zhu, W. Liu, D. Zhao, Q. Hao, J. Li, J. Huang, L. Wang, Label-Free Electrochemical
414 Sensing Platform for MicroRNA-21 Detection Using Thionine and Gold Nanoparticles Co-
415 Functionalized MoS₂ Nanosheet, *ACS Appl. Mater. Interfaces* 9 (2017) 35597-35603.
416 <https://doi.org/10.1021/acsami.7b11385>
- 417 [52] W.-J. Guo, Z. Wu, X.-Y. Yang, D.-W. Pang, Z.-L., Ultrasensitive electrochemical
418 detection of microRNA-21 with wide linear dynamic range based on dual signal amplification,
419 *Biosens. Bioelectron.* 131 (2019) 267-273. <https://doi.org/10.1016/j.bios.2019.02.026>

- 420 [53] S. Su, W. Cao, W. Liu, Z. Lu, D. Zhu, J. Chao, L. Weng, L. Wang, C. Fan, L. Wang, Dual-
421 mode electrochemical analysis of microRNA-21 using gold nanoparticle-decorated MoS₂
422 nanosheet, *Biosens. Bioelectron.* 94 (2017) 552-559.
423 <https://doi.org/10.1016/j.bios.2017.03.040>
- 424 [54] J. Wang, J. Lu, S. Dong, N. Zhu, E. Gyimah, K. Wang, Y. Li, Z. Zhang, An ultrasensitive
425 electrochemical biosensor for detection of microRNA-21 based on redox reaction of ascorbic
426 acid/iodine and duplex-specific nuclease assisted target recycling, *Biosens. Bioelectron.* 130
427 (2019) 81-87. <https://doi.org/10.1016/j.bios.2019.01.031>
- 428 [55] J. Lu, J. Wang, X. Hu, E. Gyimah, S. Yakubu, K. Wang, X. Wu, Z. Zhang, Electrochemical
429 Biosensor Based on Tetrahedral DNA Nanostructures and G-Quadruplex-Hemin
430 Conformation for the Ultrasensitive Detection of MicroRNA-21 in Serum, *Anal. Chem.* 91
431 (2019) 7353-7359. <https://doi.org/10.1021/acs.analchem.9b01133>
- 432 [56] N. Xia, X. Wang, D. Deng, G. Wang, H. Zhai, S.J. Li, Label-Free Electrochemical Sensor
433 for MicroRNAs Detection with Ferroceneboronic Acids as Redox Probes, *Int. J. Electrochem.*
434 *Sci.* 8 (2013) 9714-9722. <https://doi.org/10.1002/elan.201300077>
- 435 [57] P. Jolly, M.R. Batistuti, A. Miodek, P. Zhurauski, M. Mulato, M.A. Lindsay, P. Estrela,
436 Highly sensitive dual mode electrochemical platform for microRNA detection, *Sci. Rep.* 6
437 (2016) 36719. <https://doi.org/10.1038/srep36719>
- 438 [58] G. Yammouri, J. Mandli, H. Mohammadi, A. Amine, Development of an electrochemical
439 label-free biosensor for microRNA-125a detection using pencil graphite electrode modified
440 with different carbon nanomaterials, *J. Electroanal. Chem.* 806 (2017) 75-81.
441 <https://doi.org/10.1016/j.jelechem.2017.10.012>
- 442 [59] Z. Liang, D. Ou, D., Sun, Y. Tong, H. Luo, Z. Chen, Ultrasensitive biosensor for
443 microRNA-155 using synergistically catalytic nanoprobe coupled with improved cascade
444 strand displacement reaction, *Biosens. Bioelectron.* 146 (2019) 111744.
445 <https://doi.org/10.1016/j.bios.2019.111744>
- 446 [60] F. Wang, Y. Chu, Y. Ai, L. Chen, F. Gao, Graphene oxide with in-situ grown Prussian
447 Blue as an electrochemical probe for microRNA-122, *Microchim. Acta* 186 (2019) 116.
448 <https://doi.org/10.1007/s00604-018-3204-9>
- 449 [61] B. Jeong, Y.J. Kim, J.-Y., Jeong, Y.J. Kim, Label-free electrochemical quantification of
450 microRNA-375 in prostate cancer cells, *J. Electroanal. Chem.* 846 (2019) 113127.
451 <https://doi.org/10.1016/j.jelechem.2019.05.009>

452
453
454
455
456
457
458

459 **The list of figure captions:**

460

461 **Figure 1.** SEM images of (a,b) unmodified paper electrode and (c,d) AuNPs modified paper
462 electrode at magnification of 20000× and 50000x.

463 **Figure 2.** The concept of AuNPs modified paper electrode sensing system. Left, the sketch of
464 the paper electrode sensing system. AuNP deposition is performed by chronoamperometry in
465 15 mM HAuCl₄ aqueous solution by applying -0.3 V constant potential during 600 s. **(I)** CVs
466 of PE and AuNP-PE. Supporting electrolyte solution is 0.1 M KCl containing 50 mM
467 [Fe(CN)₆]³⁻. **(II)** Nyquist diagrams of PE and AuNP-PE. Supporting electrolyte solution is 0.1
468 M KCl containing 5 mM [Fe(CN)₆]^{3-/4-}.

469 **Figure 3.** **(A)** Nyquist diagrams obtained before / after hybridization of probe with 0.5, 1, 1.5,
470 2 µg/mL miRNA 155 target. **(B)** The calibration graph obtained after hybridization between 0.5
471 µg/mL miRNA 155 DNA probe and miRNA 155 target with its various concentrations from 0
472 to 1.5 µg/mL (n=3).

473 **Figure 4.** Selectivity of AuNP-PE. Histograms representing the average R_{ct} values obtained by
474 (a) miRNA 155 probe/AuNP-PE, hybridization between probe and (b) miRNA 155, (c) non-
475 complementary (NC), (d) single-base mismatched strand (MM), and mixture samples with (e)
476 miRNA 155 and NC or (f) miRNA 155 and MM strand (n=3).

477 **Figure 5.** **(A)** Nyquist diagrams obtained before / after hybridization of probe with 2, 4, 6
478 µg/mL miRNA 155 in 1:400 diluted FBS medium. **(B)** The calibration graph based on average
479 R_{ct} values obtained after hybridization between probe and miRNA 155 with its various
480 concentrations from 0 to 4 µg/mL in 1:400 diluted FBS medium (n=3).

481

482

483

484

485

486

487

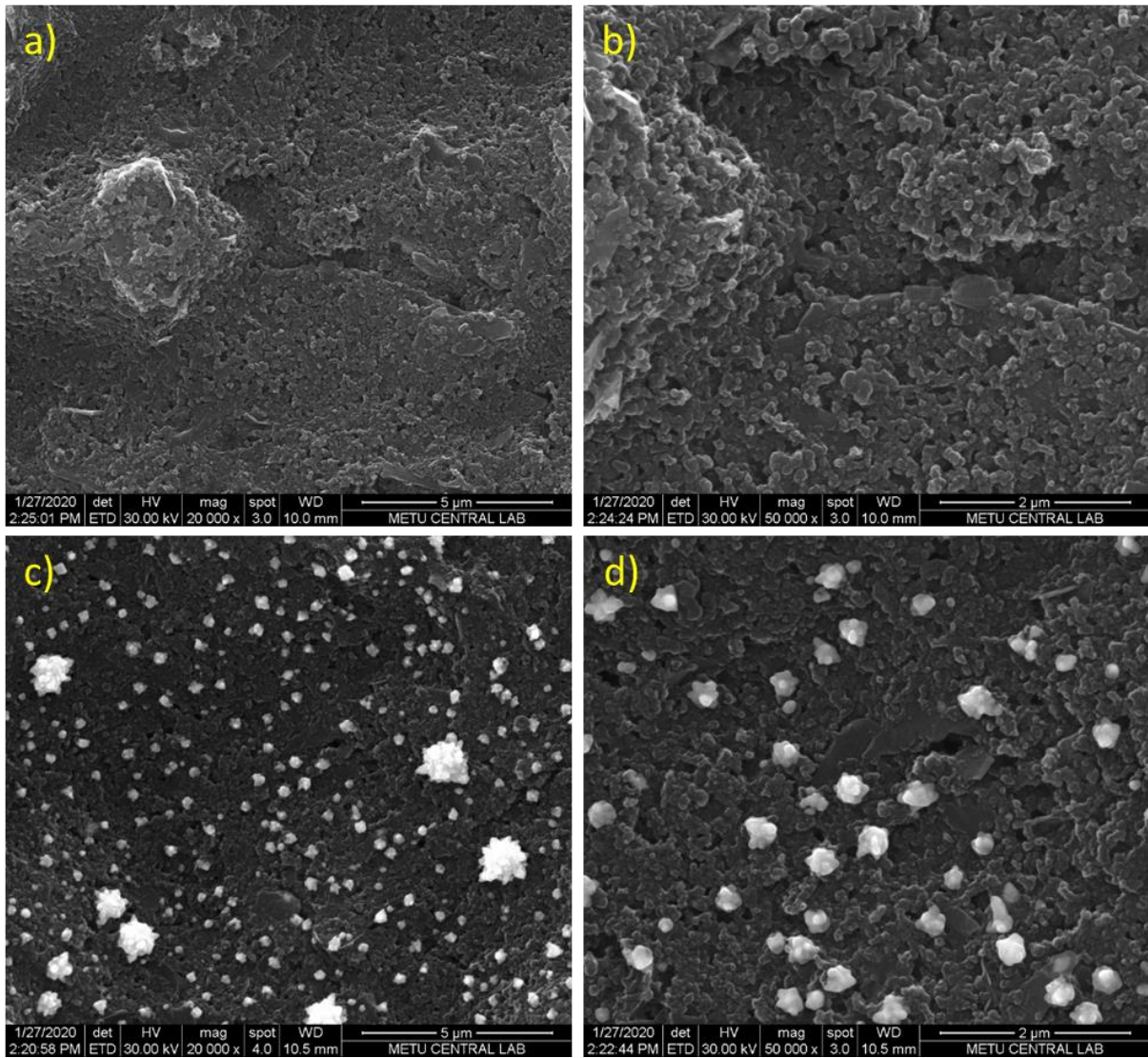
488

489

490

Figures

491

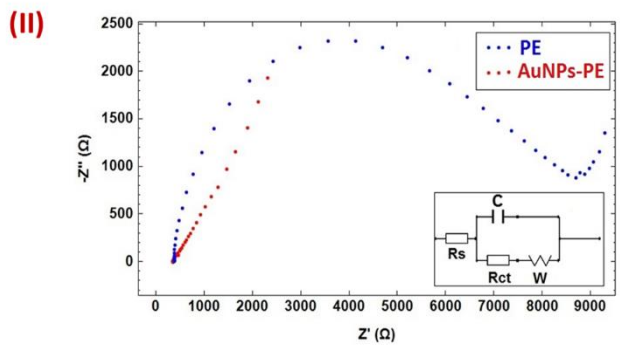
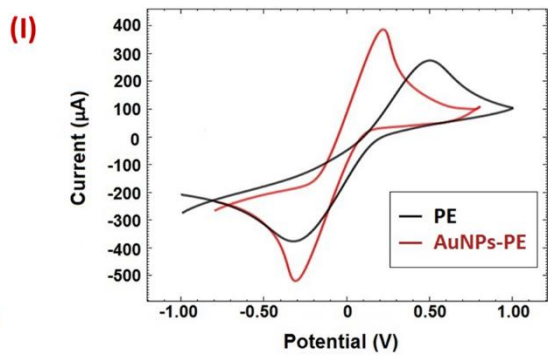
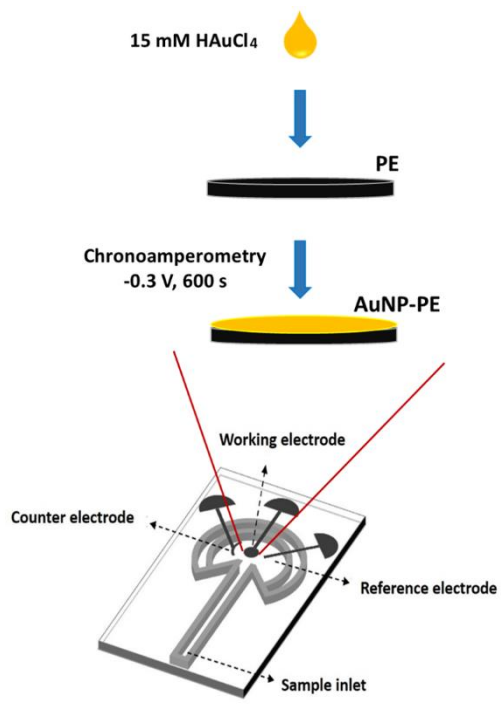


492

493

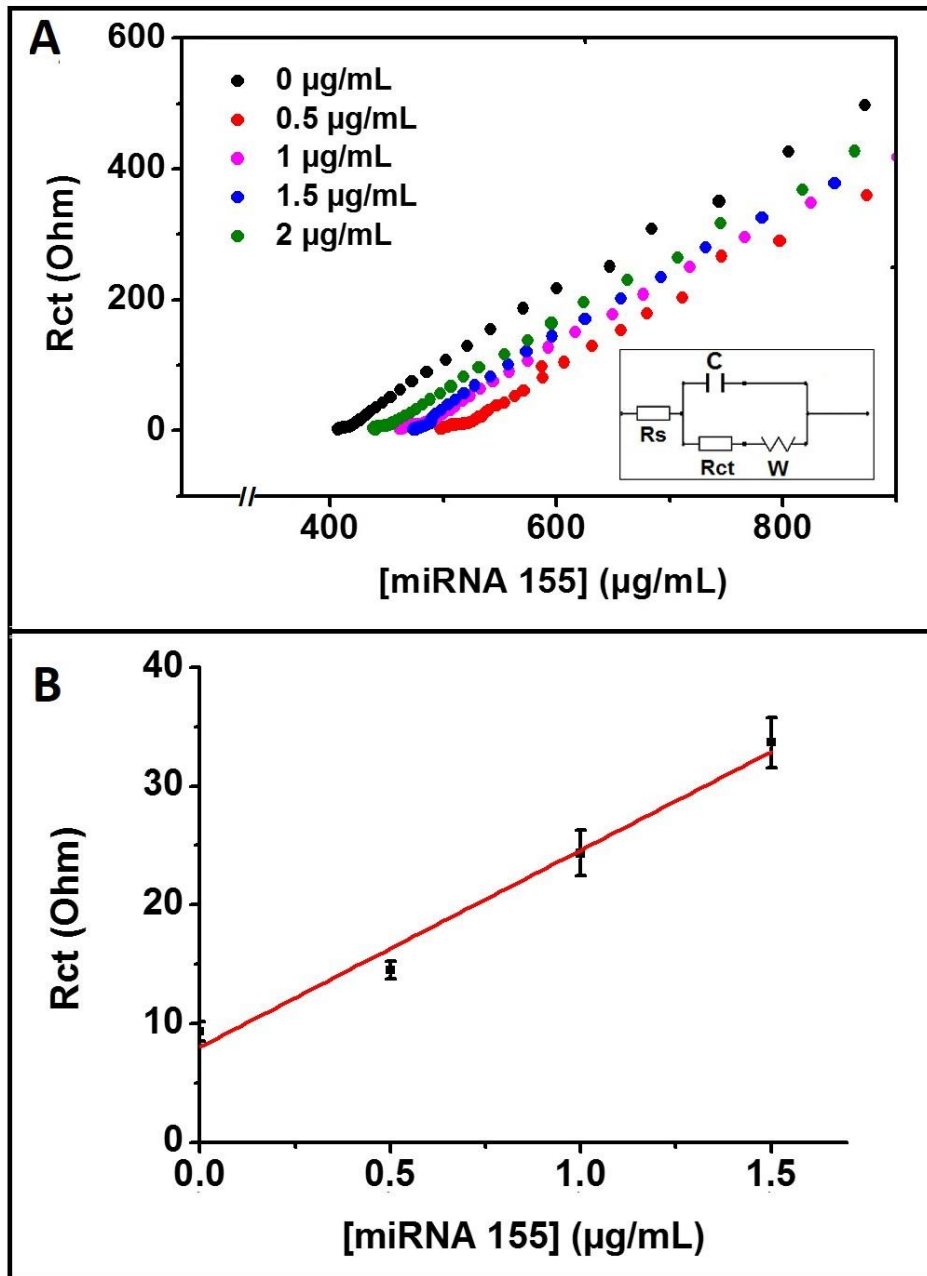
Figure 1.

494



495
496

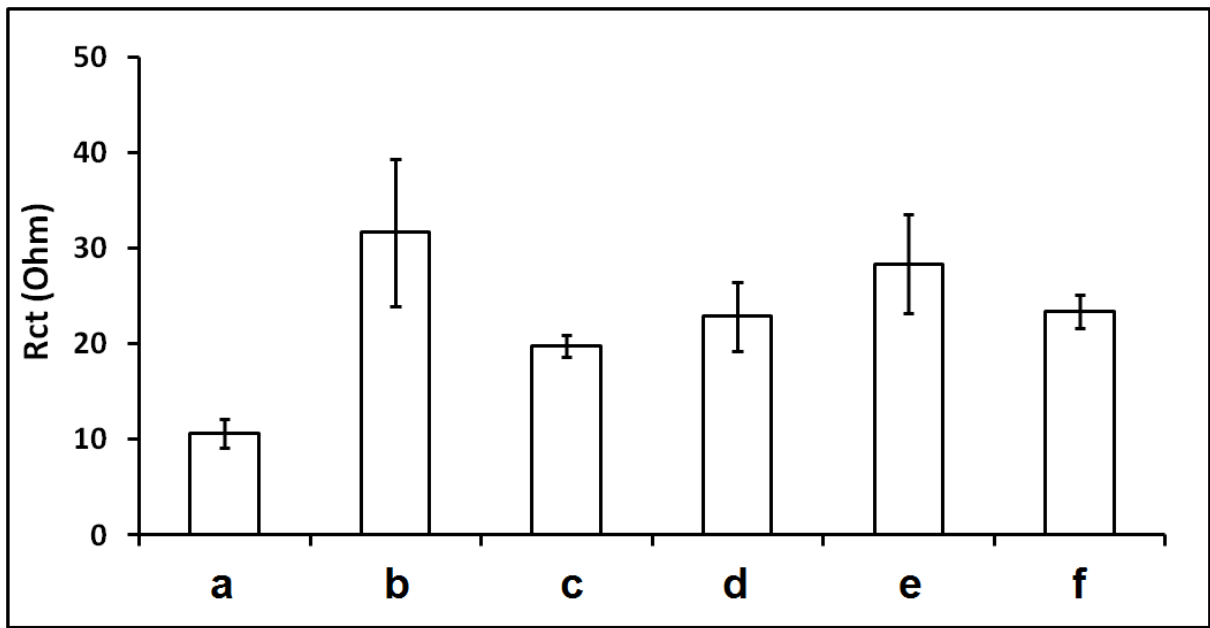
Figure 2.



497

498

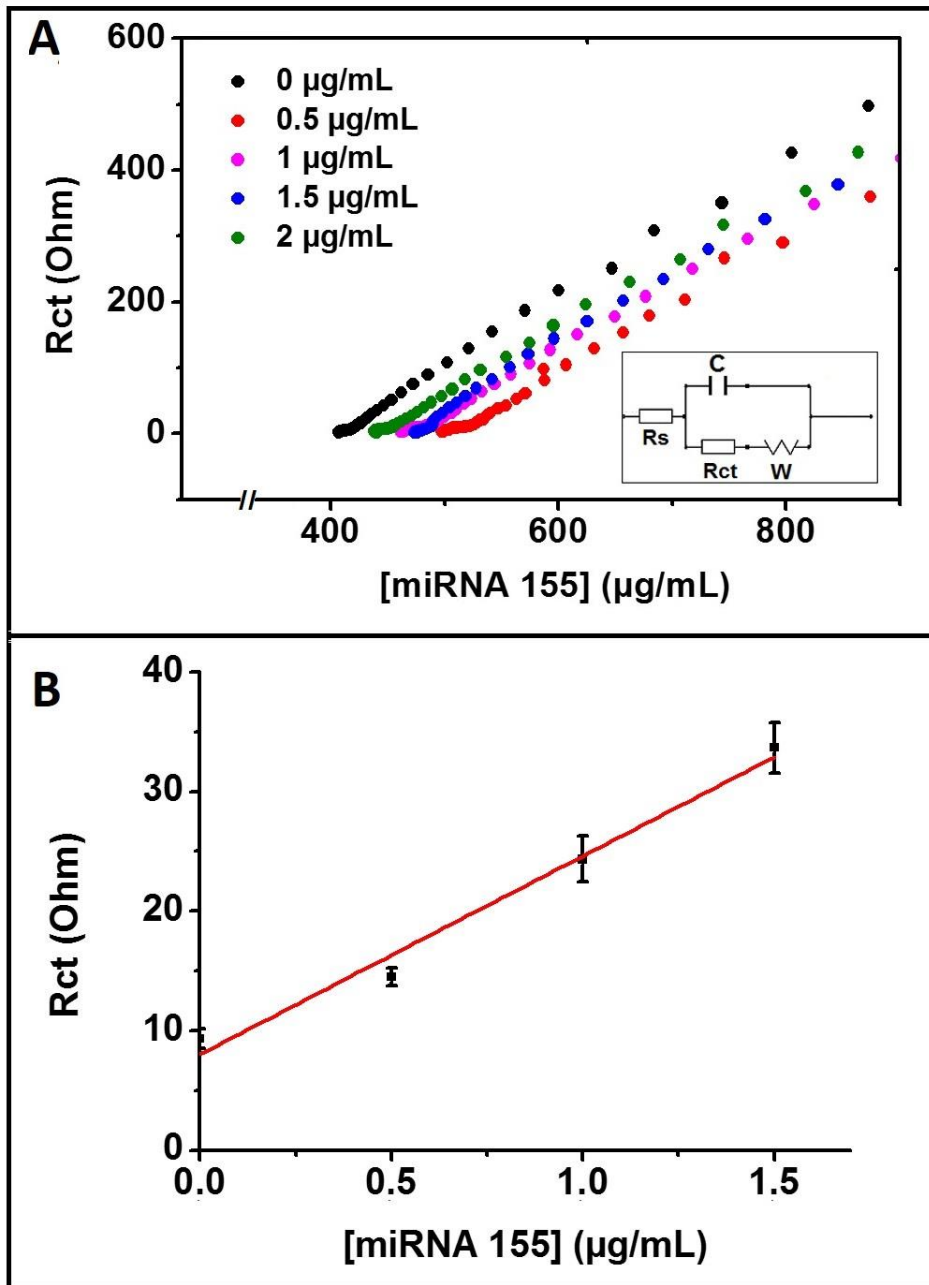
Figure 3.



499

500

Figure 4.



501

502

503

Figure 5.